Comparison of sensors and techniques for crop yield mapping [1]

Stuart J. Birrell [a,*], Kenneth A. Sudduth [b], Steven C. Borgelt [a]

[a] *Department of Agricultural Engineering, University of Missouri, Columbia, MO 65211, USA*
[b] *USDA-Agricultural Research Service, University of Missouri, Columbia, MO 65211, USA*

Abstract

The implementation of site-specific crop management is dependent on the variations in yield and yield potential within a field. Crop yield maps are important for both the implementation and evaluation of site-specific crop management strategies. Management decisions and evaluations based on yield maps must take into consideration the accuracy and resolution of the maps.

An impact-based yield monitor and a volumetric yield monitor were compared. The effect of different dynamic models of combine grain flow on the calculated instantaneous yields were investigated. Both simple time delay models and first order models could be used to model the grain flow. In general, a simple time delay model with minimal smoothing provided the best yield maps. Yield maps developed using different methods of Kriging and other mapping techniques were compared. The maps showed the same general trends. However, localized yield features were represented differently due to the methods used for developing the maps and the degree of smoothing.

Keywords: Yield monitor; Mapping; Kriging; Precision agriculture

1. Introduction

The implementation of spatially selective field operations is dependent on mapping within-field variations in soil and crop parameters (Stafford et al., 1991). Crop yield maps provide important information for developing strategies for site-specific

---

crop management. The recommendation rates for many inputs are influenced by yield goal, which in turn may be estimated from previous yield maps. Additionally, yield maps are a necessary tool in the agronomic and economic assessment of site-specific crop management.

Recently, continuous grain flow monitors have been used in conjunction with speed sensors and location systems to map crop yield (Colvin et al., 1991; Vansichen and De Baerdemaeker, 1991; Schnug et al., 1992; Auernhammer et al., 1993; Birrell et al., 1993). Searcy et al. (1989) and Vansichen and De Baerdemaeker (1991) both suggested modelling the grain flow through the combine as a first order system with a time lag, to relate the grain flow measured at the grain tank to the yield of the crop entering the combine head. The development of grain yield maps requires that instantaneous grain yields be averaged or interpolated to obtain an estimate of the average yield within a certain area.

Since yield maps may be used both for the determination of management inputs and to evaluate the results of management strategies, it is important to consider the accuracy of mapped data. Decisions based on the magnitude of the yield within cells must not only consider the yield estimates within each cell but also the reliability of those estimates, and whether any differences in estimates are significant or merely a result of the uncertainty present in the estimates. The unit cell size and the mathematical methods used to generate the maps can have a significant effect on the uncertainty of the estimate. While increasing the unit cell size or increasing the amount of smoothing will result in the loss of information about short range variability in actual yield, the uncertainty in the estimate of the average yield within a cell will be reduced.

2. Objectives

The objectives of the work reported were:

(1) to compare the operation of a volumetric-based grain yield monitor to an impact-based yield monitor;

(2) to investigate the results obtained by using different combine grain flow models to determine instantaneous grain yield;

(3) to analyze the effect of different Kriging parameters on the mapping of grain yield; and

(4) to compare yield maps developed using data from evenly spaced transects with maps developed using data obtained from the entire field.

3. Equipment and instrumentation

Two instrumented combines, a three-row John Deere 3300 and a six-row Gleaner R62, were used to collect yield data within the same field. The field was located in north-central Missouri, on claypan soils belonging to the Alfisol soil order, formed from loess over glacial till. The field was planted to corn on a 0.762-m row spacing. The combine yield mapping systems consisted of four components:

(1) Global Positioning System (GPS) receivers to determine combine location;

(2) a combine-mounted grain flow sensor;

(3) a sensor to measure ground speed; and

(4) a data acquisition system.

In addition, a weigh bin mounted in the grain tank of the John Deere combine was used to measure accumulated grain for sensor calibration. The Gleaner combine was not equipped with a weigh bin. Therefore, the accumulated grain mass was determined for calibration by weighing the grain truck before and after the combine bin was emptied into the truck. A DMC moisture sensor was installed on each combine to measure grain moisture content. Two Ashtech M-XII GPS receivers were used to provide location data. The receivers were used in the post-process C/A code differential mode (Harrison et al., 1992).

The John Deere 3300 three-row combine was equipped with a volumetric Claydon Yieldometer (Searcy et al., 1989). This yield sensor measured the volume flow of grain from the clean grain elevator. A capacitive level sensor controlled the rotation of a six-flight paddle wheel to maintain the level of grain above the paddle within an adjustable deadband. When grain levels rose above the high threshold the paddle wheel began to rotate at a constant speed, continuing until the low threshold was reached and the paddle stopped rotating. The Yieldometer was modified by replacing the standard two counts/revolution sensor connected to the shaft of the paddle wheel with an angular position encoder (1024 counts/revolution). Ground speed and distance travelled were measured using a Dickey-john radar gun.

The Gleaner R62 combine was instrumented with an impact-based AgLeader Yield Monitor 2000. This sensor measured the force of the grain impacting against a plate situated at the top of the clean grain elevator. The force, elevator speed and other measured parameters were then used within the Yield Monitor 2000 to determine grain mass flow rate. The AgLeader system included a monitor which displayed instantaneous values and cumulative totals of yield, grain moisture, grain flow, speed, distance and other parameters. Although only cumulative totals were stored for each load of grain, yield parameters were also output to a serial port at 1-s intervals. The factory-installed magnetic pick-up speed sensor was used to determine combine speed and distance travelled.

The two combine data acquisition systems relied on portable computers running essentially the same software. The computer received the uncorrected GPS position and GPS time through one serial port. In the John Deere combine, the analog and digital signals from the moisture sensor, volumetric yield sensor and speed sensor were input to an IOtech Daqbook data acquisition system and transferred to the computer through the parallel port. The impact-based yield monitor on the Gleaner logged its output to the computer through a serial port. All data was recorded at 1-s intervals.

4. Procedures

The radar gun and volumetric yield sensor on the John Deere combine were calibrated by flagging the beginning and end of a transect of known distance, while collecting the grain in the weigh bin situated in the combine clean grain tank.

This was repeated several times and a linear least squares regression was used to calibrate the recorded counts to distance ($r^2 = 0.998$, $n = 142$) and accumulated grain mass ($r^2 = 0.997$, $n = 77$).

The magnetic pickup on the Gleaner combine was calibrated prior to harvest by travelling along a known distance at normal harvest speeds. The grain flow rate measurement was calibrated by comparing the accumulated grain mass (kg load^{-1}) recorded by the impact-based monitor to the total mass of grain unloaded into the grain truck ($r^2 = 0.993$, $n = 22$).

The vehicle speed and distance used in the calculation of yields were determined from the radar gun (John Deere) and magnetic pickup (Gleaner), and GPS positions were only used for location. Since the optimum operating speeds for the two combines were different, the Gleaner combine operated at a mean speed of 2.5 m s^{-1} while the John Deere operated at only 1 m s^{-1}.

The John Deere combine with the volumetric monitor was used to harvest a pair of transects every 100 m at the same locations as those harvested the previous year. The remainder of the corn field was harvested using the Gleaner combine instrumented with an impact-based monitor.

The nominal accuracy of the GPS system used was 1–3 m. The actual accuracy obtained during the field tests was estimated by comparing the instantaneous positions recorded every second to the mean of the recorded positions, during the time when the combine was known to be stationary. The two-sigma GPS error during this period was approximately 2 m. This method of error determination actually provided a measure of the precision of the GPS measurements and not the accuracy of the measurements. The determination of absolute accuracy would require a second more accurate location system, which was not available during this harvest, to compare with the GPS measurements used. However, a reasonable estimate of the accuracy of the system could be obtained, provided the stationary time periods were sufficiently long that the mean of the recorded positions was a reasonable estimate of the true position.

5. Data analysis

For yield mapping, the measured grain flow at the sensor must be related to the rate of grain flow into the combine head. The rate of grain flow into the combine head can then be related to the yield since the velocity, swath width and position of the combine are known. If the combine system dynamics are modelled as a simple time delay, then the yield can be calculated directly by dividing the measured grain flow at any instant of time (t) by the area covered t_p seconds previously. For discrete sampling, the yield can be expressed as

$$y(i - t_p/T - t_s/2T) = \frac{\displaystyle\sum_{j=1-t_s/T}^{i} f(j)}{\displaystyle\sum_{k=i-t_p/t-t_s/T}^{i-t_p/T} d(k)} \times \frac{1000}{w} \tag{1}$$

The delay time is t_p, and t_s is the time interval over which a running average yield is calculated.

In the time domain, a continuous first order system is expressed as

$$f(t) = r(t)\left(1 - \exp((t - t_p - t_o)/\tau)\right) \tag{2}$$

The first order system can be written in the Laplace domain (Franklin and Powell, 1980). The Laplace function must then be transformed to the z domain since the data collection process is discrete. There are different methods to convert to the z transform, but the step-invariant transform is probably the most appropriate, since entering the crop is approximately a step input. The step-invariant transform is calculated by adding a zero order hold transform to the Laplace transfer function and then converting to the z transform. The discrete difference form of the z transform of this system is

$$r(i - t_p/T - 1) = \frac{1}{(1 - e^{-T/\tau})} \times \left(f(i) - e^{-T/\tau} f(i - 1)\right) \tag{3}$$

Due to the on/off method of operation of the volumetric yield monitor, raw yield counts did not accumulate with every reading (taken on 1-s intervals), even when there was continuous grain flow into the yield monitor. The volumetric monitor itself acted as a sample-and-hold system. This system exhibited a varying time constant since the interval between successive rotations was a function of flow rate. Since successive rotations generally occurred within 3 s, the original raw data was modified to obtain a single reading every 3 s by accumulating the yield counts over 3-s intervals.

Instantaneous yields were calculated from the raw impact-based monitor data (kg s^{-1}) and the modified volumetric monitor data using both a simple time delay model (Eq. 1) and a first order system model (Eq. 3), with different time delays and time constants, and with varying amounts of smoothing applied to the grain flow rate and velocity data inputs. Grain flow rate and velocity inputs were smoothed using a running average with smoothing times ranging from 0 to 21 s. The mean combine time delay was estimated by comparing the time at which the combine head entered or exited the crop, to the time at which the measured grain flow began or stopped. The different time delays (8–15 s) used in the simple time delay and first order models spanned the mean estimated time delay (10 s). The first order models were tested using time constants ranging from 0.3 to 4 s.

The correlations between the instantaneous yields of a particular transect, calculated using different models were determined by comparing yields on a point-by-point basis along the transect. The correlations were determined for all of the transects harvested using the John Deere, and for the adjacent transects harvested by the Gleaner. The John Deere combine with the volumetric yield monitor was used to harvest six pairs of transects spaced evenly across the field. The 12 adjacent transects harvested by the Gleaner combine with the impact-based monitor were identified and used for comparison.

Yield maps can be developed using many different interpolation methods, including the arithmetic means, inverse distance weighing methods and Kriging.

Generally, due to the continuous determination of the instantaneous yield, the different methods will result in similar maps being developed. However, Kriging is the only method which estimates both the value at a given location and the variance for the interpolated value. This variance of the estimate is important to distinguish whether the yields in two cells are significantly different from each other or if the difference in the estimated values is a result of the variance in estimation. Therefore, the main advantage of Kriging is that both an estimate of the interpolated value and an indication of the reliability of that estimate are given.

Calculated instantaneous yields were checked for normality and then exported to a geostatistical package (GS + Geostatistics for Biological Sciences version 2.1, Gamma Design Software) for analysis and the development of yield maps by universal block Kriging (Webster, 1985). The Kriged results from the different models were used to develop maps over the field with identical cell sizes (10×10 m). The support for the sample variogram was approximately $10 \ m^2$ for the impact-based monitor and $2 \ m^2$ for the volumetric yield monitor (Webster, 1985). When the input data sets included all of the yield transects collected over the field, the Kriging parameters were set to restrict the number of nearest neighbours to a maximum of 8 or 24, which increased the degree of smoothing. When the six pairs of transects were used to generate the map, 32 neighbours were used to decrease the "striping" effect caused by the much higher sampling intensity in the direction of the rows.

The above methods all involved complicated post-processing operations and yield maps could only be generated after collection of all the data. Another mapping method was based on a real-time graphical display of the yield map which could be obtained during harvesting. The limits of the field were used to size a graphical window on the computer screen. As the data was collected, the instantaneous yields were calculated using a simple time delay model and the pixels on the screen representing the harvested area were painted with a colour representing the instantaneous yield, provided that the calculated yield and instantaneous velocity were greater than some threshold value. Each pixel represented an area of approximately $3 \ m^2$. However, if in subsequent passes, the threshold conditions were met and the harvested location corresponded to a pixel previously harvested, the pixel was repainted and the old information lost. To compare this map to the Kriged yield maps, the pixels contained within each 10 m grid cell in the field were combined to obtain a mean yield for the cell.

The previous analyses all required the calculation of instantaneous yields, which were then averaged to obtain the mean yield for each unit cell. However, if the instantaneous mass of grain collected at each location was accumulated in the relevant cell, it would not be necessary to calculate instantaneous yield. In this method, the geographical harvested area corresponding to each sample point was determined geometrically from the GPS location coordinates. The grain mass was then distributed to each grid cell traversed according to the ratio of the harvested area in any particular grid cell to the total area harvested for each sample point. Although it was still necessary to model the grain flow dynamics (simple time delay used) to locate the position from which the grain was harvested, the effects of sudden changes in velocity on the data were reduced by not calculating instantaneous yields.

6. Results and discussion

While the average yields determined with the two monitors on adjacent transects were similar, the calculated instantaneous yields from the impact-based monitor showed considerably less noise than yields obtained from the volumetric monitor (Figs. 1 and 2). The greater noise was primarily due to the discrete operation of the volumetric yield monitor, whereas the impact-based monitor more closely approximated a continuous sampling system. The correlation between the accumulated yield and batch weights was very high for both the volumetric monitor ($r^2 = 0.997$, $n = 78$) and impact-based sensor ($r^2 = 0.993$, $n = 23$).

The instantaneous yield for the impact-based monitor was calculated using different models (Fig. 1). When a simple time delay model was used, the calculated instantaneous yield showed little noise, little or no smoothing of the raw data was needed to discern the shape of the instantaneous yield curve, and further smoothing resulted in the loss of information on the short range variability. However, when a
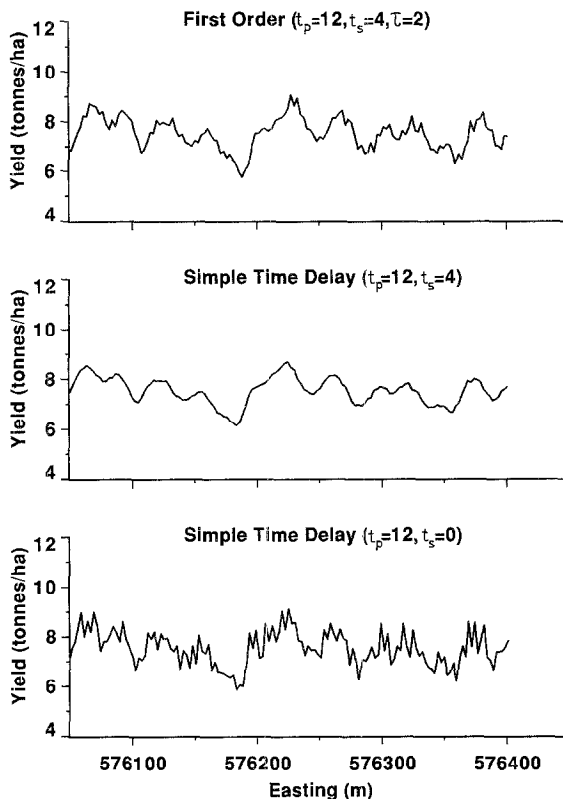

Fig. 1. Yield calculated from impact-based yield monitor data, using a first order model and simple time delay model with two smoothing times. (Time delay $t_p = 12$ s; smoothing time $t_s = 0$–4 s; first order system time constant $\tau = 2$ s.)
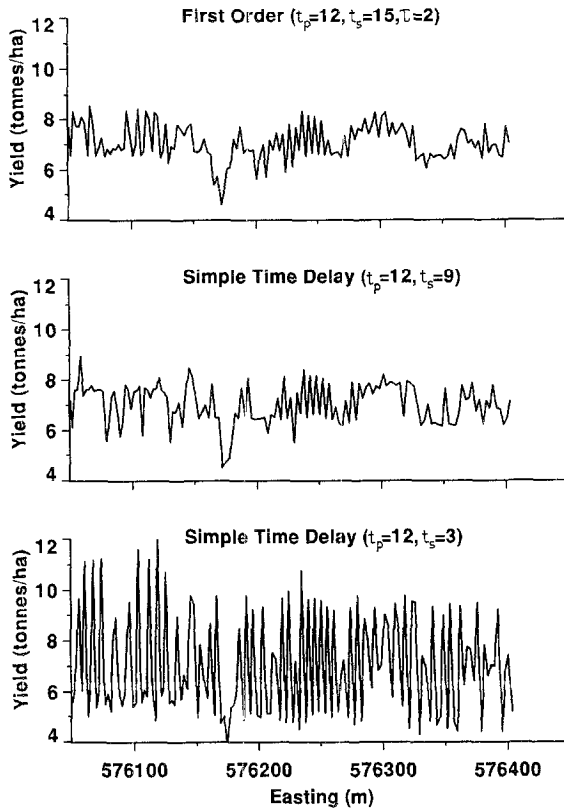
Fig. 2. Yield calculated from volumetric yield monitor data, using a first order model and simple time delay model with two smoothing times. (Time delay t_p = 12 s; smoothing time t_s = 3–15 s; first order system time constant τ = 2 s.)

first order model was used without smoothing, the calculated yield displayed a high frequency noise component due to the amplification of the highest frequencies in the raw data caused by the inversion of the first order system. The high frequency component in the raw data was most likely a result of unsteady grain flow through the combine. However, it was not possible to identify the frequency at which the changes in calculated instantaneous yield were a result of true changes in yield. When the raw data was smoothed, the calculated yield from the first order system approached that obtained from a simple time delay model (Fig. 1). The smoothed first order and simple time delay model yields were very similar except when entering the crop, where the first order delay model more closely modelled the step change in yield. However, since the yields calculated were unreliable when a large change in velocity occurred, and should probably be disregarded, there may be little advantage in more accurately modelling this step change in yield.

The instantaneous yield for the volumetric monitor was calculated using various models (Fig. 2). The simple time delay model showed a substantial amount of noise

with no smoothing of the modified raw data, but smoothing allowed the local trends in yield to be seen (Fig. 2). When a first order system was used, the high frequency noise began to dominate the signal, even with smoothing of the model input data. This was caused by the discrete operation of the monitor. Theoretically, the monitor could be modelled as an additional first order system. However, the time constant of this model would vary with yield, adding another unknown parameter to the system model.

The correlation coefficients between the instantaneous yields obtained using the different models were calculated for each transect and for all the transects together (Table 1). Since harvesting is a destructive test, it was not possible to measure the actual yield and then harvest the same area using a yield monitor for comparison. Therefore, it was impossible to determine the true instantaneous yield and it was necessary to rely on the correlation between the different calculation methods to determine which methods were superior. If the correlation for one method was very sensitive to the parameters used, such as the smoothing time and time constant, then that method must be considered with some suspicion. The impact-based monitor showed a high correlation between simple time delay models with different smoothing intervals. The correlation between yield estimates using a first order system with no smoothing and the simple delay models was low. However, the correlation improved with increased smoothing of the first order models. The correlation decreased as the time constant was increased (Table 1). The volumetric monitor showed similar trends, except the degree of smoothing required to improve the correlation was much greater. The first order systems showed considerable high frequency noise, which was reflected in the lower correlations between the models (Table 1).

The calculated instantaneous yields data from the impact-based monitor was normally distributed. The calculated instantaneous yield did not have significant outliers since the computation algorithm discarded calculated yields beyond certain threshold values to account for discontinuities in harvest speed which results in large spikes in calculated yield if the combine suddenly stopped. The calculated instantaneous yield from the volumetric-based monitor was normal when the raw data was highly smoothed. However, for unsmoothed data the instantaneous yields departed from a normal distribution due to the discrete operation of the sensor, which resulted in a flattening of the peak of the distribution curve.

The yield semi-variograms were highly dependent on the type of yield monitor and the combine model. The best fit semi-variograms for the different combine models, using the volumetric monitor data, were linear semi-variograms that displayed a high nugget variance or pure nugget semi-variograms (Webster, 1985). The simple time delay and first order models for the impact-based monitor exhibited either exponential or spherical semi-variograms, with a definite spatial range (Fig. 3). Although the shapes of the semi-variograms were similar, the first order models exhibited a much higher nugget variance than the simple time delay variograms. The increase in nugget variance was a reflection of the introduction of the high frequency noise components in the calculated instantaneous yields.

The complete set of raw harvest data from the impact-based monitor was used to generate yield maps, using different combine models and Kriging parameters. A

Table 1
Correlation coefficient between a selected reference model and the simple time delay (SD) and first order (FO) combine models with different degrees of smoothing [time delay (t_p) = 12 s; time constant (τ) = 2 or 3 s; smoothing time (t_s) = 0–21 s]

Transect	1A	1B	2A	2B	3A	3B	4A	4B	5A	5B	6A	6B	1A–6B
Impact-based monitor: correlation of different models with simple time delay model with no smoothing (SD t_p = 12 s, t_s = 0 s)													
SD t_p = 12 s, t_s = 0 s	1.00	1.00	1.00	1.00	1.00	1.00	1.00	1.00	1.00	1.00	1.00	1.00	1.00
SD t_p = 12 s, t_s = 4 s	0.92	0.94	0.74	0.94	0.97	0.93	0.89	0.94	0.94	0.95	0.96	0.91	0.92
FO t_p = 12 s, t_s = 0 s, τ = 2 s	0.08	0.16	-0.31	0.09	0.56	0.22	0.09	0.26	0.23	0.32	0.34	0.22	0.19
FO t_p = 12 s, t_s = 4 s, τ = 2 s	0.67	0.72	0.45	0.74	0.86	0.70	0.48	0.71	0.74	0.73	0.68	0.63	0.68
FO t_p = 12 s, t_s = 0 s, τ = 3 s	-0.11	-0.04	-0.41	-0.11	0.39	0.03	-0.06	0.08	0.03	0.11	0.11	0.03	0.00
FO t_p = 12 s, t_s = 4 s, τ = 3 s	0.37	0.45	0.30	0.48	0.79	0.53	0.32	0.58	0.54	0.56	0.44	0.47	0.49
Volumetric monitor: correlation of different models with simple time delay model with 15-s smoothing (SD t_p = 12 s, t_s = 15 s)													
SD t_p = 12 s, t_s = 3 s	0.41	0.51	0.49	0.25	0.16	0.44	0.53	0.35	0.46	0.56	0.46	0.44	0.42
SD t_p = 12 s, t_s = 15 s	1.00	1.00	1.00	1.00	1.00	1.00	1.00	1.00	1.00	1.00	1.00	1.00	1.00
SD t_p = 12 s, t_s = 21 s	0.83	0.94	0.93	0.66	0.64	0.92	0.93	0.47	0.89	0.95	0.94	0.90	0.83
FO t_p = 12 s, t_s = 3 s, τ = 2 s	0.30	0.44	0.44	0.05	0.15	0.28	0.41	-0.12	0.38	0.38	0.48	0.35	0.30
FO t_p = 12 s, t_s = 15 s, τ = 2 s	0.65	0.86	0.82	0.39	0.37	0.84	0.85	0.15	0.82	0.86	0.86	0.72	0.68
FO t_p = 12 s, t_s = 3 s, τ = 3 s	0.24	0.35	0.36	0.02	0.12	0.20	0.32	-0.15	0.30	0.29	0.42	0.28	0.23
FO t_p = 12 s, t_s = 21 s, τ = 3 s	0.80	0.93	0.88	0.78	0.72	0.89	0.88	0.76	0.86	0.91	0.87	0.84	0.84

Adjacent pairs of transects are identified with the same number and letters distinguish between individual transects within each combine pair.
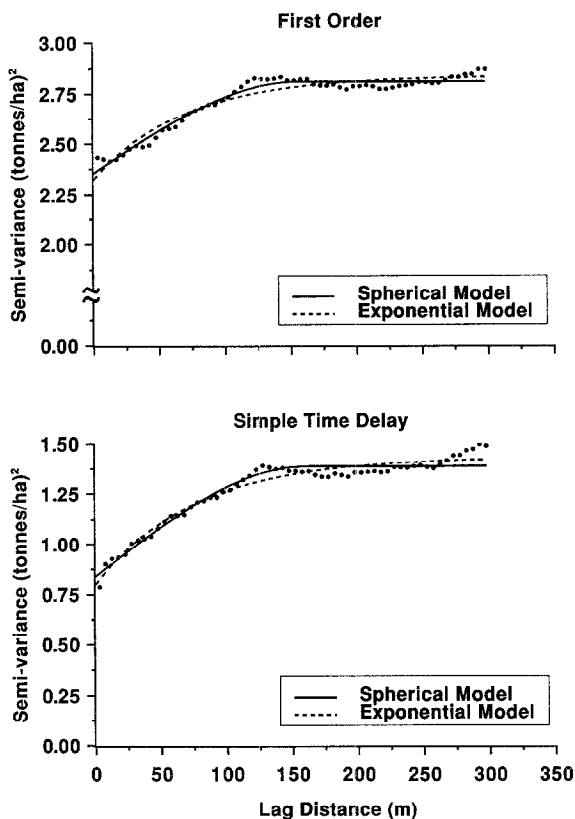
Fig. 3. Yield semi-variograms calculated from impact-based yield monitor data: (top) first order model, no smoothing; and (bottom) simple time delay model, no smoothing.

simple time delay model with no smoothing (Fig. 4a, b) and a first order model with no smoothing (Fig. 4c, d) were used. Two different sets of Kriging parameters were used to vary the spatial smoothing of the yield maps:

(1) maximum lag of 300 m and the number of points used for the calculation of a grid cell restricted to 24 closest neighbours (Fig. 4a, c);

(2) maximum lag of 100 m and the number of points used for the calculation of a grid cell restricted to eight closest neighbours (Fig. 4b, d).

The general yield trends were the same for all of the maps. When the number of neighbours used in the Kriging process was reduced, the trends did not change but the displayed local variability increased, as shown in Fig. 4. When a first order system was used the maps showed a much higher yield along the edge of the field than when a simple time delay model was used, due to the step response of the first order system. However, the calculated yields appeared to be higher than the actual yields in these areas, and the error associated with the calculation of the instantaneous yield at these transition points was high.

100 m

5.25 6.00 6.75 7.50 8.25
tonnes/ha
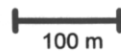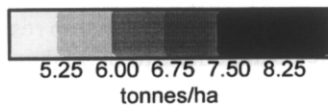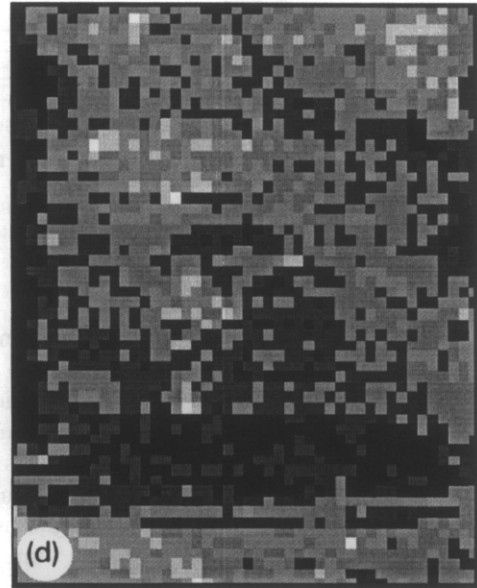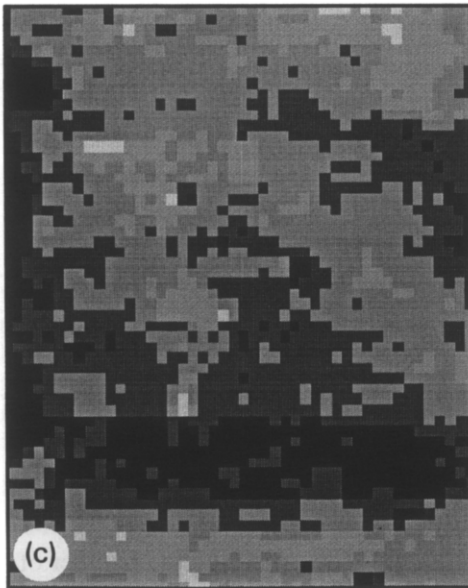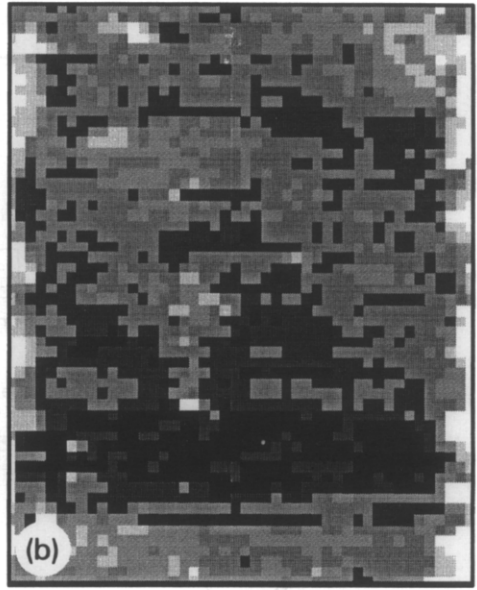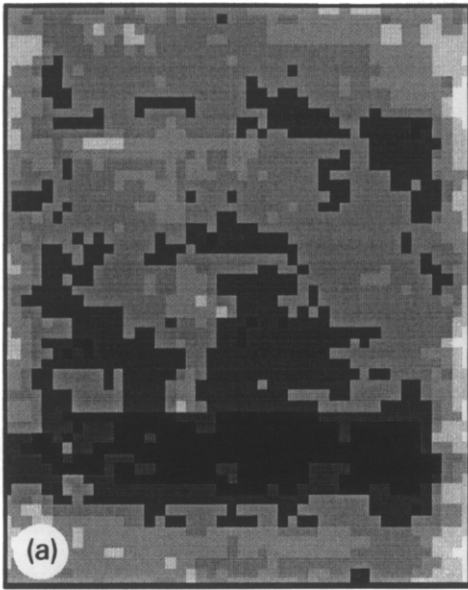
The main advantage of Kriging is that the mean square error values, or Kriging variances (Fig. 5), are calculated for each interpolated value (Fig. 4). The Kriging variance for the simple time delay maps was much lower than the respective Kriging variance for the first order models. Decreasing the number of neighbours used in the Kriging process from 24 neighbours (Fig. 5a, c) to eight neighbours (Fig. 5b, d) increased the Kriging variance. Although decreasing the number of neighbours results in maps showing greater local variability, the uncertainty associated with those estimates increases. This increases the probability of incorrectly identifying two cells as having different mean yields.

Data from six pairs of transects 100 m apart harvested by the Gleaner combine with the impact-based monitor were used to generate a map utilizing a simple time delay model with 4-s smoothing (Fig. 6a). While much of the fine detail was lost, the general trends were very similar to those previously shown (Fig. 4). Data from adjacent pairs of transects harvested by the John Deere combine with the volumetric monitor were also used to generate a map, using a simple time delay model and 15-s smoothing (Fig. 6b). Although further detail was missing, the basic trends were the same. Although there were some differences between the maps developed from transects and those developed from a complete set of data, the transect maps provided a reasonable representation of yield trends. However, the accuracy of transect-based maps would also be dependent on the location and direction of the transects relative to important changes in yield.

The on-screen map generated during harvesting (Fig. 7a) was remarkably similar to the Kriged maps and clearly showed the same trends, although some information was lost due to repainting of the screen, especially along the edge of the field. When the mean yields for each 10 m grid cell were mapped (Fig. 7b), the resulting map showed almost identical trends to those found on the Kriged maps (Fig. 4). While this method shows promise, the critical factor that determines the accuracy of the map is the level of the yield and velocity thresholds below which the pixels are not repainted. The velocity thresholds are a function of the "normal" operating velocity, while the yield threshold will depend on both the type of crop and the actual yield of the field being harvested.

The map generated by the accumulation of the grain mass in each grid cell (Fig. 8) displayed the same general trends but with greater local variability perpendicular to the direction of travel. This was due to the high ratio of position error to grid cell size which increased the probability of identifying the incorrect cell. This effect could be minimized by increasing cell size or reducing the error in position location.

The correlations between the various maps were compared on a cell-by-cell basis (Table 2). All of the whole-field simple time delay models exhibited a high degree of correlation with each other. The unsmoothed first order system exhibited a low

Fig. 4 (left). Yield maps developed from impact-based monitor data. Simple time delay model with no smoothing: (a) Kriging 300 m and 24 neighbours; (b) Kriging 100 m and eight neighbours. First order model with no smoothing: (c) Kriging 300 m and 24 neighbours; (d) Kriging 100 m and eight neighbours.

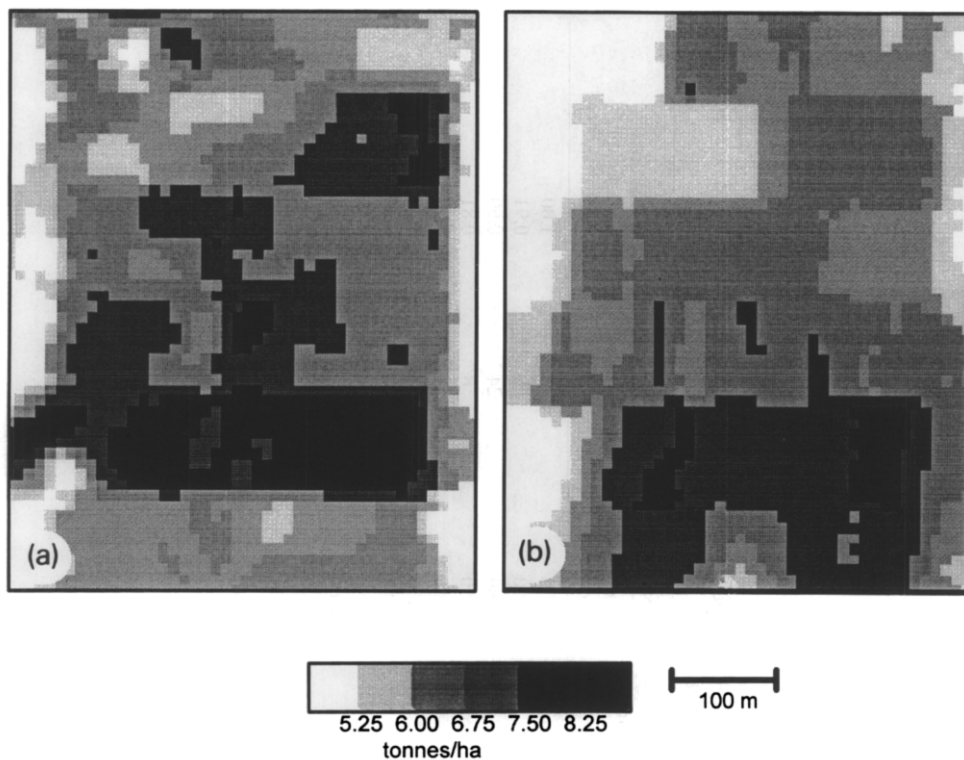0.25 0.35 0.45 0.55 0.65

tonnes/ha

100 m
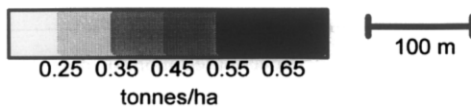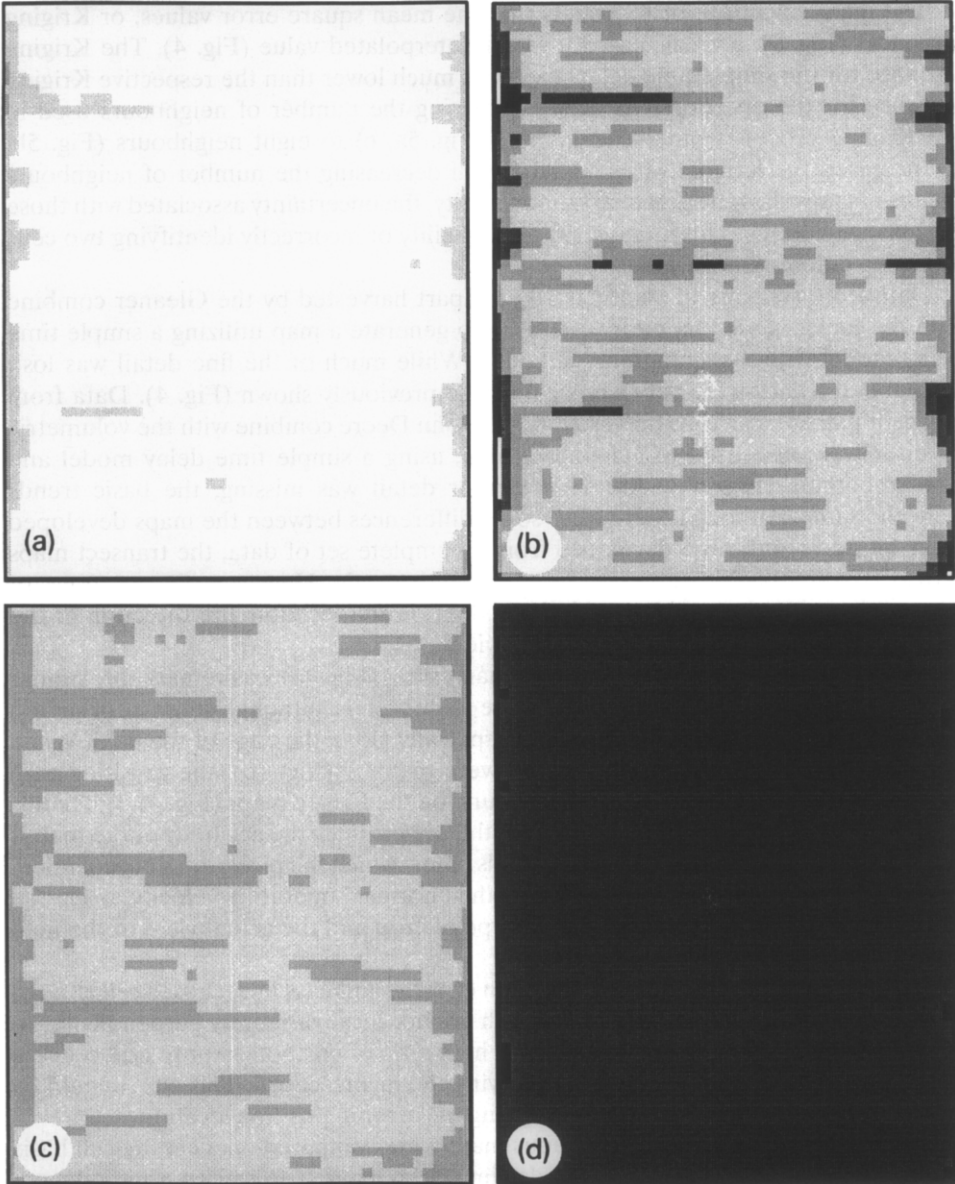
Fig. 6. Yield maps developed using six pairs of transects. (a) Impact-based monitor, simple time delay model with 4-s smoothing; (b) volumetric monitor data using a simple time delay model with 15-s smoothing.

correlation when compared to the simple time delay maps, due to the high frequency components introduced. The transect maps developed from the impact-based monitor were reasonably well-correlated to the maps from the whole field data, but the volumetric-based monitor transects showed a lower correlation. The lower correlation for the volumetric-based monitor transects was due to the increase in the amount of smoothing required, which removed the yield variation over short distances. In general, it appears that a simple time delay model with minimal smoothing provided the best yield maps. However, maps generated from evenly spaced transects showed the general yield trends and would provide useful information. The maps developed using the graphical method and grid accumulation method were not highly correlated

Fig. 5 (left). Maps of standard deviation of Kriging variance developed from impact-based monitor data. Simple time delay model with no smoothing: (a) Kriging 300 m and 24 neighbours; (b) Kriging 100 m and eight neighbours. First order model with no smoothing: (c) Kriging 300 m and 24 neighbours; (d) Kriging 100 m and eight neighbours.

Table 2
Correlations calculated for Kriged maps developed with different combine models and Kriging parameters (compared to map from Gleaner combine data with a simple delay model, no smoothing, 24 neighbours and 300 m active Kriging range)

| Data source	Model type	Smoothing (s)	Time constant (s)	Kriging parameters		
				Semi-variogram active range (m)	Number of neighbours	Correlation coefficient
Gleaner (all data)	Simple time delay	0		300	24	1.00
Gleaner (all data)	Simple time delay	0		100	8	0.91
Gleaner (all data)	Simple time delay	4		300	24	0.90
Gleaner (all data)	Simple time delay	4		100	8	0.81
Gleaner (all data)	First order system	0	2	300	24	0.58
Gleaner (all data)	First order system	0	2	100	8	0.49
Gleaner (all data)	First order system	4	3	300	24	0.68
Gleaner (all data)	First order system	4	3	100	8	0.61
Gleaner (transects)	Simple time delay	4		300	32	0.64
JD 3300 (transects)	Simple time delay	15		300	32	0.41
JD 3300 and Gleaner	Graphical display					0.42
JD 3300 and Gleaner	Mass accumulation					0.48
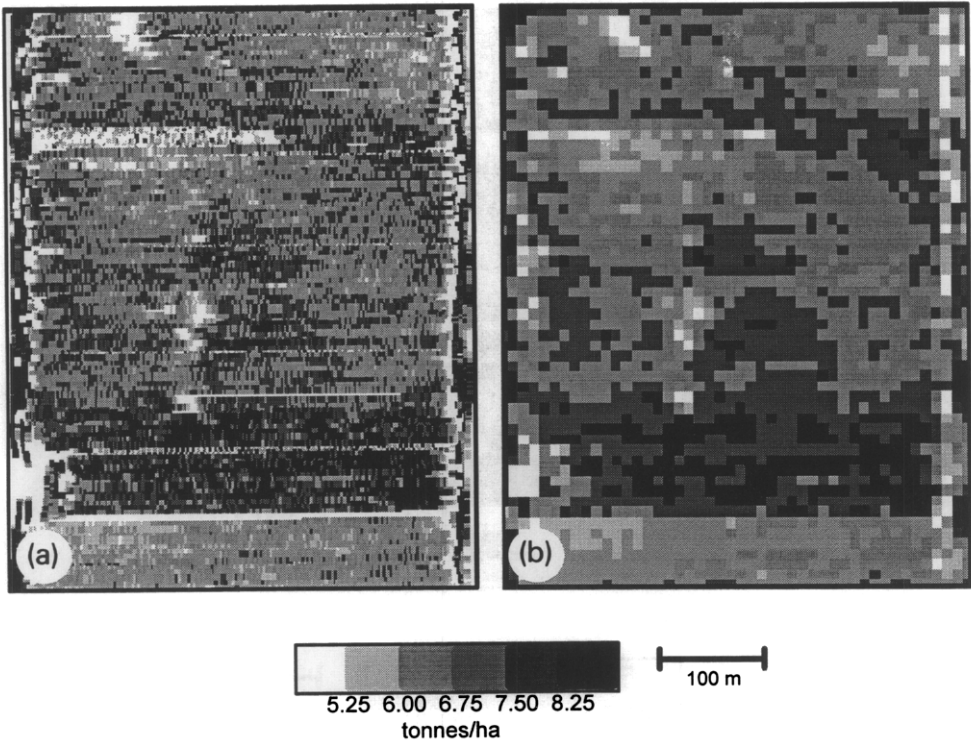
Fig. 7. Yield maps developed using graphical method. (a) On-screen yield map during harvesting, simple time delay model; (b) transformation of on-screen map to a 10 m grid.

to the Kriged maps ($r^2 = 0.42$ and 0.48, respectively). While the graphical methods were not highly correlated to the Kriged maps, the graphical method would be useful for a real-time display during harvest and for visual comparisons of yield to other factors.

7. Summary

The impact-based sensor and the volumetric yield monitor both showed a very high correlation with the batch weights ($r^2 > 0.99$). However, the discrete operation of the volumetric monitor introduced significant errors in the calculation of instantaneous yield. The impact-based sensor more closely approximated a continuous sampling system, which minimizes the potential problems of discrete sampling and the potential for aliasing. The volumetric yield monitor would be greatly improved if the on/off control of the paddle wheel were replaced by some form of proportional controller, to more closely approximate a continuous sampling system.

Simple time delay and first order models both appeared to be reasonable approaches to modelling combine flow dynamics. The simple time delay model was less
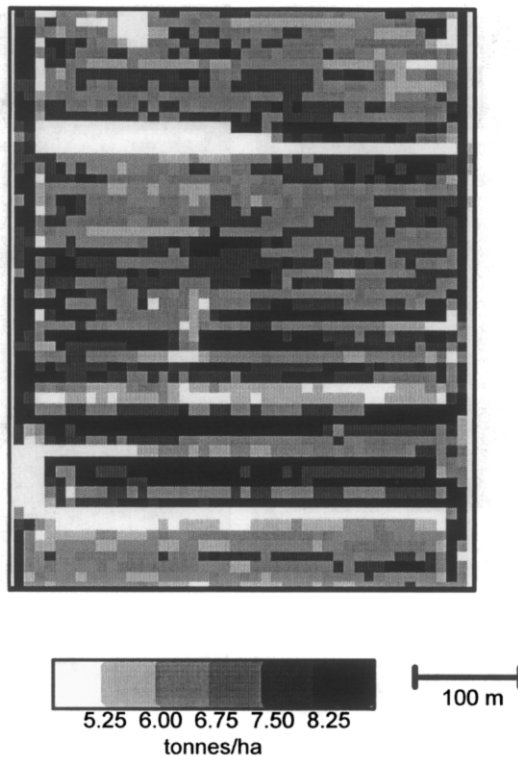
Fig. 8. Yield map generated by the accumulation of grain mass in each grid cell.

susceptible to noise but did not accurately model the step change in yield seen when entering or exiting a crop. The first order system modelled the step yield input but was highly susceptible to noise and required smoothing of the raw data. Overall, the simple time delay model was better than the first order model.

The Kriging of instantaneous yield to develop maps was fairly robust if a complete data set was used. The general trends in the data were evident even when cell values were calculated from a very localized region. Evenly spaced transects could be used to develop maps showing general yield trends although some detail was lost. While a visual comparison of all the maps showed the same trends, the statistical correlations between some maps were relatively low, which suggests that the grid cell size should probably be increased to improve confidence in mean yields for individual cells.

Acknowledgement

Nomenclature table

$y(t)$ Grain yield at combine head at time t (kg ha^{-1})
$f(t)$ Grain flow through yield monitor at time t (kg s^{-1})
$r(t)$ Grain flow entering combine head at time t (kg s^{-1})
$v(t)$ Velocity of combine at time t (m s^{-1})
t_o Time combine started harvesting
t_p Delay time (s)
t_s Smoothing period (s)
T Sampling period (s)
τ First order system, time constant
w Swath width (m)
$y(i)$ Calculated yield at combine head at time t, over period T, $i = t/T$ (kg ha^{-1})
$f(i)$ Measured grain flow through yield monitor over period T (kg s^{-1})
$r(i)$ Calculated grain flow entering combine head over period T (kg s^{-1})
$d(i)$ Measured distance travelled over time period T (m)

References

Auernhammer, H., Demmel, M., Muhr, K., Rottmeier, J. and Wild, K. (1993) Yield measurements on combine harvesters. ASAE Paper 93-1506.

Birrell, S.J., Sudduth, K.A. and Borgelt, S.C. (1993) Crop yield mapping using GPS. ASAE Paper MC93-104.

Colvin, T.S., Karlen, D.L. and Tischer, N. (1991) Yield variability within fields in central Iowa. In: Proceedings ASAE Symposium on Automated Agriculture for the 21st Century, 16–17 Dec., 1991, Chicago, Ill. American Society of Agricultural Engineers, St. Joseph, Mich., pp. 336–373.

Franklin, G.F. and Powell, J.D. (1980) Digital Control of Dynamic Systems. Addison-Wesley Publishing Co., Reading, Mass., 335 pp.

Harrison, J.D., Birrell, S.J., Sudduth, K.A. and Borgelt, S.C. (1992) Global positioning system applications for site-specific farming research. ASAE Paper 92-3615.

Schnug, E., Murphy, D., Evans, E., Haneklaus, S. and Lamp, J. (1992) Yield mapping and application of yield maps to computer-aided local resource management. In: P.C. Robert, R.H. Rust and W.E. Larson (Editors), Proceedings of the Workshop on Research and Development Issues on Soil Specific Crop Management, April 14–16, 1992, Minneapolis, Minn. American Society of Agronomy, Madison, Wisc., pp. 87–93.

Searcy, S.W., Schueller, J.K., Bae, Y.H., Borgelt, S.C. and Stout, B.A. (1989) Mapping of spatially variable yield during grain combining. Trans. ASAE, 32(3): 826–829.

Stafford, J.V., Ambler, B. and Smith, M.P. (1991) Sensing and mapping grain yield variations. In: Proceedings ASAE Symposium on Automated Agriculture for the 21st Century, 16–17 Dec., 1991, Chicago, Ill. American Society of Agricultural Engineers, St. Joseph, Mich., pp. 356–364.

Vansichen, R. and De Baerdemaeker, J. (1991) Continuous wheat yield measurement on a combine. In: Proceedings ASAE Symposium on Automated Agriculture for the 21st Century, 16–17 Dec., 1991, Chicago, Ill. American Society of Agricultural Engineers, St. Joseph, Mich., pp. 346–355.

Webster, R. (1985) Quantitative spatial analysis of soil in the field. Adv. Soil Sci., 3: 1–70.